



**NURC**

a NATO Research Centre  
un Centre de Recherche de l'OTAN



PARTNERING  
FOR MARITIME  
INNOVATION

Reprint Series

NURC-PR-2008-005

# Target detection and location with ambient noise

Chris H. Harrison

September 2008

Originally published in:

Journal of the Acoustical Society of America, Vol. 123, No. 4, April 2008,  
pp. 1834-1837.

## About NURC

### *Our vision*

- To conduct maritime research and develop products in support of NATO's maritime operational and transformational requirements.
- To be the first port of call for NATO's maritime research needs through our own expertise, particularly in the undersea domain, and that of our many partners in research and technology.

One of three research and technology organisations in NATO, NURC conducts maritime research in support of NATO's operational and transformation requirements. Reporting to the Supreme Allied Commander, Transformation and under the guidance of the NATO Conference of National Armaments Directors and the NATO Military Committee, our focus is on the undersea domain and on solutions to maritime security problems.

The Scientific Committee of National Representatives, membership of which is open to all NATO nations, provides scientific guidance to NURC and the Supreme Allied Commander Transformation.

NURC is funded through NATO common funds and respond explicitly to NATO's common requirements. Our plans and operations are extensively and regularly reviewed by outside bodies including peer review of the science and technology, independent national expert oversight, review of proposed deliverables by military user authorities, and independent business process certification.



**Copyright © Acoustical Society of America, 2008.**

**NOTE:** The NURC Reprint series reprints papers and articles published by NURC authors in the open literature as an effort to widely disseminate NURC products. Users should cite the original article where possible.

# Target detection and location with ambient noise (L)

Christopher H. Harrison<sup>a)</sup>

NATO Undersea Research Centre, Viale San Bartolomeo, 400, 19126 La Spezia, Italy

(Received 28 September 2007; revised 17 January 2008; accepted 17 January 2008)

By placing a vertical array in an ambient noise field and forming an upward and a downward beam one obtains two time series which can be cross correlated to reveal a subbottom profile of the seabed [Siderius *et al.*, *J. Acoust. Soc. Am.* **120**, 1315–1323 (2006)]. Here the cross-correlation approach is applied to the location in range and bearing of a point target. An experiment was designed using floats and weights mounted (and dismounted) on the same cable as the vertical array. Careful measurements were made of the location of all likely floats, ballast weights, array terminations, and so on. After suitable coherent averaging, peaks were seen at delays (correlation offsets) agreeing with the reflector positions and were shown to be absent when reflectors were removed. A trivial extension of the theory developed in Harrison and Siderius [*J. Acoust. Soc. Am.* **123**, 1282–1296 (2008)] is used to explain the rough amplitudes of the reflections. The approach differs from “acoustic daylight” principally in having a capability to determine a target range.

© 2008 Acoustical Society of America. [DOI: 10.1121/1.2872516]

PACS number(s): 43.30.Pc, 43.30.Nb, 43.30.Gv, 43.30.Jx [RCG]

## I. INTRODUCTION

The cross correlation of the time series received on a pair of hydrophones in a noise field is closely related to the impulse response that would be received on replacing one of them by a sound source. A relationship was established by Weaver and Lobkis (2004) and has since been developed in underwater acoustics by Roux and Kuperman (2004), Roux *et al.* (2005), Sabra *et al.* (2004), and Sabra *et al.* (2005). More recently it was demonstrated by Siderius *et al.* (2006) that the process could be used to survey subbottom layering with a moving vertical array. The correlation peak is caused by a small area of sea surface sources immediately above the array from which an almost identical wave form passes, first directly to the array, then to the seabed, and back to the array. The steered vertical beams cut out a large part of the ineffective, uncorrelated noise but retain contributions from this small area. By this reasoning one might also expect to see a reflection from a point scatterer (target) under, or at least, below the center line of the array. In fact, some circumstantial evidence for this has already been pointed out in Harrison and Siderius (2008) where correlation peaks at round-trip path lengths of about 20 m from the array were attributed to a reflection from a ballast weight mounted beneath the array. In principle, taking account of surface noise reflected from the seabed, both target and array are surrounded by sources, so targets above the array ought to be just as detectable. In practice, these would require much longer integration times to eliminate the competing direct and much louder surface noise. Laboratory passive imaging of objects has already been demonstrated using a single ultrasonic receiver and autocorrelation (Larose *et al.*, 2006). In principle, underwater subbottom profiling or target detection would also be possible with a single hydrophone (in effect,

the hydrophone and its image in the seabed can be thought of as a pair), but integration times would be prohibitive.

In a recent experiment (CLUTTER 2007) the exact positions of the array elements, ballast, array termination, and so on were measured. In addition, on a separate occasion three hollow glass sphere floats were mounted between the array and the ballast weight. Thus all conceivable reflectors above and below the array were controlled. This letter reports the successful detection and ranging of these targets. To be precise there are correlation peaks where there are known scatterers below the array and no peaks where there are no scatterers. In addition, there are no peaks corresponding to the delays of the floats above the array, which agrees with expectations since the sound sources are predominantly at the surface.

Although this is not the first demonstration of target detection with noise, this approach is novel in resolving the target range, and it operates like a passive radar. In this respect it is quite distinct from acoustic daylight (Buckingham *et al.*, 1992; Potter, 1994; Epifanio *et al.*, 1999) which, being an analogue of daylight vision, resolves a two-dimensional angle. The passive radar range resolution is dependent on the bandwidth and is not particularly dependent on frequency. Its angle resolution just depends on the array size, and in principle, the cross-correlation process still functions with a single hydrophone, though with complete absence of angle resolution. Also, in principle, the weakest target can still be detected even though it sits in a noise field, provided it does not move and given long enough integration time.

## II. THEORY

A recent paper (Harrison and Siderius, 2008) developed a formula for the correlation peak height given by a plane reflector and checked it against simulations and experimental results (BOUNDARY2003 and BOUNDARY2004) using a cross-correlation normalization that would result in a peak height of unity if the two arriving time series were identical.

<sup>a)</sup>Electronic mail: harrison@nurc.nato.int

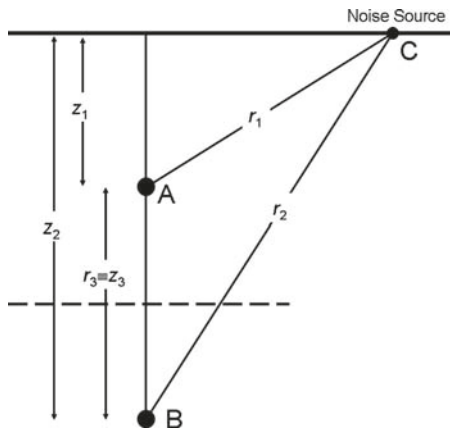


FIG. 1. Geometrical construction to convert existing horizontal plane reflection formulas for use with point targets. Ray paths associated with an arbitrary noise source  $C$  on the sea surface and the locations  $A$  and  $B$  are shown.  $A$  represents the receiving array, and the direct path has length  $r_1$ . In the reflection case,  $B$  is interpreted as the image of  $A$  in a horizontal plane reflector (dashed line), and the complete reflected path  $CB$  has length  $r_2$ . In the target scattering case,  $B$  is interpreted as a point target (in the absence of the plane reflector), and the complete scattered path  $CBA$  has length  $r_2 + r_3$ .

With this normalization the result is independent of reflection coefficient magnitude since, with up and down beam time series denoted, respectively, by  $U$ ,  $D$ , the cross-correlation numerator is  $U * D$  and the denominator is the product of the standard deviations  $(\langle U^2 \rangle \langle D^2 \rangle)^{1/2}$ . Thus the magnitude of the reflection coefficient, which is contained only in  $D$ , cancels. One could just as easily have used a normalization where the denominator was  $\langle U^2 \rangle$  instead. Thus the magnitudes of the noise sources still cancel but the result does depend on the magnitude of the reflection coefficient. In the context of demonstrating a target detection it is desirable to avoid the first normalization because, although the peak height in the numerator would depend only on the target (through  $D$ ), the standard deviation of  $D$  in the denominator would also depend on reflections from the seabed. With the second normalization the resulting peak height depends only on the target.

We avoid lengthy derivations here by modifying the formula for plane reflector peak height  $P$  derived by [Harrison and Siderius \(2008\)](#) with geometry as in Fig. 1, which was

$$P_{R1} = \frac{2L \text{sign}(R)}{(z_2 - z_1) \gamma \beta}, \quad (1)$$

where  $L$  is the array length,  $\gamma$  is the ratio of sample frequency to design frequency for the array  $\gamma = f_s / f_o$ ,  $\beta$  is a numerical constant, of order unity, that depends on the array's cross-spectral density matrix and shading,  $R$  is reflection coefficient, and  $z_1$ ,  $z_2$  are the respective depths of the array (center) and its image in the seabed.

With the second type of normalization the formula for a plane reflector converts to

$$P_{R2} = \frac{2LR}{(z_2 - z_1) \gamma \beta}. \quad (2)$$

First we note that the path of length  $r_1$  from an arbitrary surface noise source to the array center is identical whether we consider plane reflectors or targets. [Harrison and Siderius](#)

(2008) denoted the path from the same noise source to the image receiver (in the reflection surface) as  $r_2$ . To make use of the existing formula we remove the reflector and place the target where the image used to be. (This is a mathematical construct, and has nothing to do with the physical arrangement in the experiment. The point target and plane reflector geometries are both indicated in Fig. 1.)

The path from the noise source to the target is still  $r_2$ . The remaining path from target to array is a fixed length (denoted  $r_3$ ), so from a cross-correlation point of view the geometry is the same for a target placed where the reflection image used to be except for a constant offset  $r_3$ . The original amplitude of the reflected arrival includes a spreading term  $R/r_2$  (since  $r_2$  is the complete path from source to image receiver), and this is now replaced for the target by  $s/(r_2 r_3)$  [since the source to target range is  $r_2$  and the target to receiver range is  $r_3$ , where target strength is  $\text{TS} = 20 \log_{10}(s)$ ]. Thus for a point target at depth  $z_2$  with the second normalization, noting that the depth difference  $z_3 = z_2 - z_1$ , we arrive at the formula

$$P_T = \frac{2Ls}{(z_2 - z_1)^2 \gamma \beta}. \quad (3)$$

### III. EXPERIMENTAL GEOMETRY

The experimental arrangement was a drifting 32-element vertical array with hydrophone separation 0.18 m connected by a length of cable to a radio buoy. The array was stabilized and isolated from wave motion by a 29 m length of buoyant hose forming a spar buoy. All potential targets of interest here are attached to the same cable as the array and so any vertical or horizontal motion of the array becomes unimportant. Beneath the array center there was always a solid metal termination of the array hose (approximately 0.10 m diameter) with top face at about 6.6 m, an Edgetech 8201 acoustic release between 16.3 and 17.5 m, and a ballast weight of 150 kg (a horizontal rectangular iron bar approximately 0.15 × 0.15 × 0.50 m) with its top face at 19.45 m. Because the dominant noise sources are above the array one would expect targets only to be effective below the array since their reflections are the only ones to enter the downward beam. Nevertheless there were also objects above the array that are, in principle, capable of reflection and so to avoid postexperiment uncertainty because of sidelobes, etc., their distances from array center were set so as never to coincide. In fact, there is the upper array termination at 12.6 m above array center and a pair of buoyancy glass spheres at about 75 m above.

Rather than rely on these unchanging “targets of opportunity,” in a separate experiment three Benthos 0.43-m-diam hollow glass spheres were attached to the cable (actually with their sides pressing against the taut cable) at center depths 9.64, 12.19, and 14.74 m. Their front (i.e., top) faces were therefore at depths 9.42, 11.97, and 14.52 m.

### IV. TARGET STRENGTH ESTIMATES

As a check on the strength of the various target peaks we estimate their linear target strengths  $s$ . The design frequency

of the array is 4.167 kHz, and the processing passband is between 2 and 4 kHz. Thus all acoustic wavelengths considered are greater than 0.38 m, and the targets tend to be of the order of, or smaller than, the wavelength. We consider three types of target: A horizontal rectangular iron bar, the steel end cap at the bottom of the array hose, and a hollow glass sphere.

### A. Horizontal rectangular iron bar

The iron bar has a rigid, flat, horizontal upper face whose area  $a \times b$  is smaller than the Fresnel zone so that the scattering term  $s = ab/\lambda$  (Urlick, 1975), and for the highest frequency  $s \approx 0.15 \times 0.5/0.38 = 0.20$  m.

### B. Steel end cap

Treating the end cap as a rigid disc of radius  $a = 0.045$  m we have  $s = \pi a^2/\lambda$  (Urlick, 1975) and  $s \approx 0.017$ .

### C. Hollow glass sphere

The scattering term  $s$  for a rigid sphere depends on the wave-number-radius product  $ka$  (Urlick, 1975) which in this case, with  $a = 0.215$  m, is between 1.8 and 3.6. Above  $ka = 1$  the backscattering cross section is the same as the physical cross section, so  $s$  is given by  $s = a/2 \approx 0.11$ . However, the cavity and the wall thickness of 0.014 m result in Lamb waves which enhance  $s$  by a factor between 1 and 2. On the other hand, the glass sphere is housed in a protective plastic casing that is likely to spoil this enhancement. In addition, there is a spread in arrival time caused by the Lamb wave circumnavigating the sphere many times (Tesei *et al.*, 2002). The first and strongest of these arrives a couple of meters in path length behind the arrival from the front face.

Because the depth resolution with the cross-correlation technique and this bandwidth is about 0.5 m (i.e., 1 m in path length), the spheres are resolvable at their separations of 2.55 m, so (with the possible exception of weak Lamb wave multiples) one does not need to consider addition (coherent or incoherent) of the three spheres. Nevertheless, the spheres and the ballast weight are close enough to each other to be partially obscured by the upper spheres.

## V. ACOUSTIC MEASUREMENTS AND PROCESSING

During the CLUTTER 2007 experiments in the area of the Mediterranean between Malta and Sicily several hours of ambient noise data were collected with and without the three spheres attached. The array center was at 115.6 m in the first experiment without spheres, and at 90.6 m in the second with spheres. Otherwise, cable lengths beneath the array were the same in both cases, and although the ballast weights were jettisoned, they were identical. The water depth was about 142 m depth in both cases and this ensured that competing bottom reflections were well separated in time from the desired target echoes. In fact subbottom layering, though not discussed here, has been extracted independently.

The ambient noise was sampled at 12.0 kHz and stored in files of length 131 072 samples ( $\sim 11$  s). Processing is the same as described in Harrison and Siderius (2008) for sub-

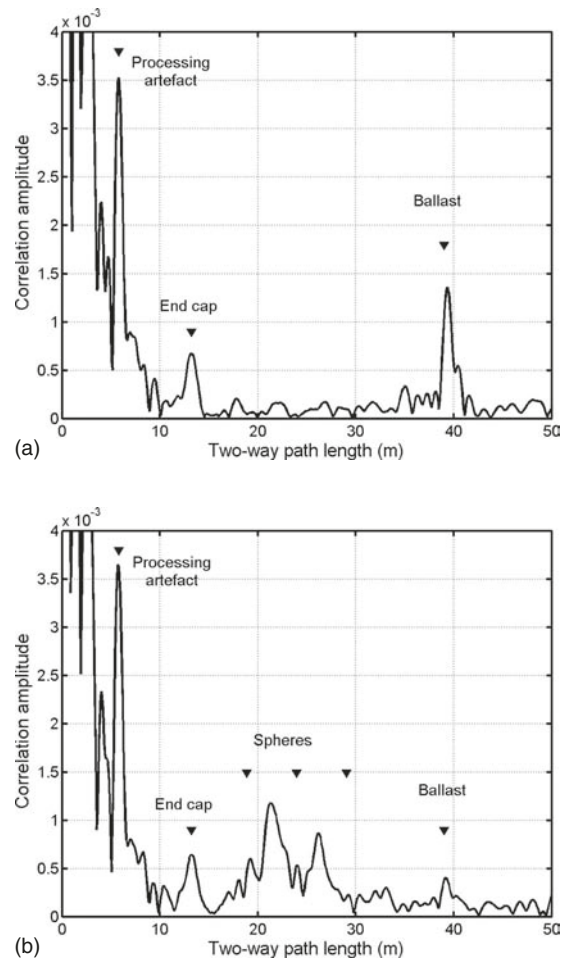


FIG. 2. Correlation amplitude, to be interpreted as an impulse response showing labeled returns (a) excluding the glass spheres and (b) including the glass spheres. Black triangles indicate measured two-way path lengths to the ballast weight, the array end cap, and the three spheres. The processing artifact corresponding to the array length is also indicated.

bottom layer extraction (namely, filter, beam form, cross correlate, differentiate). [Note that processing in Siderius *et al.* (2006) is the same except for omission of differentiation.] The processing is most efficient in the frequency domain since the filters, beam forming, cross correlation, and time differentiation can all be performed in the same operation. The only free parameter is the filter shape, and here a band-pass from half the design frequency up to the design frequency was used.

The time differentiated cross correlation of the upward and downward beam-formed time series is the impulse response, and the quantity plotted in the following graphs corresponds to the formula in Eq. (3) with  $L = 5.76$  m,  $\gamma = 2.88$ , and  $\beta = 1.87$ . The result in the first experiment with no spheres attached and coherently averaged over 600 files (approximately 100 min) is shown in Fig. 2(a). The abscissa is two-way path length assuming the measured sound speed in the vicinity of the array to be 1513 m/s. There are two clear peaks at two-way paths corresponding to the array hose termination (13.2 m) and the ballast weight (39.4 m). In between there are no significant peaks. The black triangles indicate the actual measured target positions (double their depths), and for comparison purposes, one should take the

actual acoustic peak position (rather than the leading edge) since time zero in this cross-correlation function corresponds to the central peak at zero meters. At shorter delays there is a peak corresponding to the length of the array (5.76 m), which is believed to be a processing artifact since it is enhanced by removing the beam-forming shading (Hamming) (see Gerstoft *et al.*, 2008). It is not surprising that there are large peaks at shorter delays still because the up and down beams are constructed from the same 32 hydrophones. Though not shown here, it is possible to investigate the stability of all these peaks and the reduction in the background level as the size of the average increases.

The peak height for the ballast weight is calculated using Eq. (3) with  $z_2 - z_1 = 19.5$  m and values for  $L$ ,  $s$ ,  $\gamma$ ,  $\beta$  specified earlier, as 0.0011. This is close to the actual peak height of 0.00135. Similarly, the expected peak height for the array end cap at 6.6 m away is calculated as  $0.82 \times 10^{-3}$ , and the actual peak is close at  $0.67 \times 10^{-3}$ .

With the spheres attached the result of a coherent sum over 600 files is shown in Fig. 2(b). First notice that the processing artifact at 5.76 m and the end cap return at 13.2 m are virtually identical to the earlier case. There are two additional broad peaks, each with a precursor, at two-way paths between 19 and 28 m. The position of the earliest arrival is close to that of the top face of the top sphere (shown by the left-most triangle), and the main peak is slightly later at about 21.3 m. This is believed to be the signature of a glass sphere that supports Lamb waves, possibly slightly suppressed by the plastic protective housing as discussed earlier. There is a similar but slightly weaker sequence corresponding to the second sphere starting at 23.5 m as indicated by the second black triangle. One cannot, however, see a clear return from the third sphere, but neither can one see a strong reflection from the ballast in this case. It is suspected that the first sphere has a slight screening effect. Substituting the estimated scattering term  $s$  in Eq. (3) the first sphere's peak height is calculated as 0.0027 and the second as 0.0016. The actual peaks are somewhat lower in both cases and a possible explanation is damping by the plastic cover.

## VI. CONCLUSIONS

This paper has demonstrated the detection and ranging of targets suspended underneath a vertical array using only surface ambient noise sources. The targets always included the array's ballast weight and the array hose's end cap, and on a separate occasion three glass spheres were also attached. In the absence of the spheres there was a clear reflection from the ballast and from the end cap. When the spheres were added there was a strong reflection from the first sphere, a slightly weaker return from the second, and no evidence of the third. Also, the ballast weight return was weaker, suggesting that the lower targets were partially obscured by the upper ones. This is consistent with the effective source being located at the center of the array. In contrast, the peak height for the array end cap, which was obviously closer than the other targets, was identical in both cases. In all cases the strength of the peak values was well predicted

by Eq. (3), which is adapted from an equivalent formula for plane reflectors. Equation (3) clearly shows that the strength depends only on separation of the array and target and not the positions of the noise sources.

It is important to note that this method differs from earlier acoustic daylight techniques in determining the range to the target and being more dependent on bandwidth than frequency. Its detection limits are set by the ability to discriminate one target from other target-like features rather than from noise, since the background of uncorrelated noise can be lowered without limit given enough integration time (and a stationary target and statistically stationary noise).

By coincidence in these experiments the targets were hanging under the vertical array, but there is no reason to doubt that the amplitude formula and detection should work just as well with the targets moved to one side of the vertical array axis. For practical integration times the target simply needs to be below the level of the array, so that one can draw a straight line *from* the target *through* the array *to* an area of noise sources on the sea surface. Range and intensity would be determined in exactly the same way as with a target on the vertical axis, and the normalization takes care of variation in noise source level. Angle would be resolved by the array's steered beams. By the same reasoning if angle resolution is sacrificed and there is unlimited integration time the array size can be reduced right down to a single hydrophone.

- Buckingham, M. J., Berkhout, B. V., and Glegg, S. A. L. (1992). "Imaging the ocean with ambient noise," *Nature (London)* **356**, 327–329.
- Epifanio, C. L., Potter, J. R., Deane, G. B., Readhead, M. L., and Buckingham, M. J. (1999). "Imaging in the ocean with ambient noise: The ORB experiments," *J. Acoust. Soc. Am.* **106**, 3211–3225.
- Gerstoft, P., Hodgkiss, W. S., Siderius, M., Huang, C-F., and Harrison, C. H. (2008). "Passive fathometer processing," *J. Acoust. Soc. Am.* **123**, 1297–1305.
- Harrison, C. H., and Siderius, M. (2008). "Bottom profiling by correlating beam-steered noise sequences," *J. Acoust. Soc. Am.* **123**, 1282–1296.
- Larose, E., Montaldo, G., Derode, A., and Campillo, M. (2006). "Passive imaging of localized reflectors and interfaces in open media," *Appl. Phys. Lett.* **88**, 104103-1–104103-3.
- Potter, J. R. (1994). "Acoustic imaging using ambient noise: Some theory and simulation results," *J. Acoust. Soc. Am.* **95**, 21–33.
- Roux, P., and Kuperman, W. A. (2004). "Extracting coherent wave fronts from acoustic ambient noise in the ocean," *J. Acoust. Soc. Am.* **116**, 1995–2003.
- Roux, P., Sabra, K. G., Kuperman, W. A., and Roux, A. (2005). "Ambient noise cross correlation in free space: Theoretical approach," *J. Acoust. Soc. Am.* **117**, 79–84.
- Sabra, K. G., Roux, P., and Kuperman, W. A. (2005). "Emergence rate of the time-domain Green's function from the ambient noise cross-correlation function," *J. Acoust. Soc. Am.* **118**, 3524–3531.
- Sabra, K. G., Roux, P., Kuperman, W. A., Hodgkiss, W. S., and D'Spain, G. L. (2004). "Using ocean ambient noise for array element localization," *J. Acoust. Soc. Am.* **115**, 2507 (Abstract).
- Siderius, M., Harrison, C. H., and Porter, M. B. (2006). "A passive fathometer technique for imaging seabed layering using ambient noise," *J. Acoust. Soc. Am.* **120**, 1315–1323.
- Tesei, A., Maguer, A., Fox, W. L. J., Lim, R., and Schmidt, H. (2002). "Measurements and modeling of acoustic scattering from partially and completely buried spherical shells," *J. Acoust. Soc. Am.* **112**, 1817–1830.
- Urick, R. J. (1975). "Principles of underwater sound," 2nd Ed. Chap. 7, McGraw-Hill, New York.
- Weaver, R. L., and Lobkis, O. I. (2004). "Diffuse fields in open systems and the emergence of the Green's function," *J. Acoust. Soc. Am.* **116**, 2731–2734.

# Document Data Sheet

<i>Security Classification</i>		<i>Project No.</i>
<i>Document Serial No.</i> NURC-PR-2008-005	<i>Date of Issue</i> September 2008	<i>Total Pages</i> 4 pp.
<i>Author(s)</i> Harrison, C.H.		
<i>Title</i> Target detection and location with ambient noise		
<i>Abstract</i>		
<i>Keywords</i>		
<i>Issuing Organization</i> NURC Viale San Bartolomeo 400, 19126 La Spezia, Italy  [From N. America: NURC (New York) APO AE 09613-5000]		Tel: +39 0187 527 361 Fax: +39 0187 527 700  E-mail: <a href="mailto:library@nurc.nato.int">library@nurc.nato.int</a>